Supporting Information

A pillararene-based supramolecular polymer hydrogel for removal of organic dyes from water

Jiaxin Ma[a], Shanhao Gong[b], Yujie Cheng[a], Wei Cao[a], Xuehong Wei,[a], Pi Wang[b,*], and Danyu Xia[a,*]

[a]*Scientific Instrument Center, Shanxi University, Taiyuan 030006, P. R. China*

[b]*College of Materials Science and Engineering, Taiyuan University of Technology, Taiyuan 030024, P.R. China*

[*] Corresponding authors.

E-mail address: danyuxia@sxu.edu.cn, wangpi@tyut.edu.cn

Table of Contents

1. Materials and Methods

Materials: All reagents were commercially available and used as supplied without further purification. Solvents were either employed as purchased or dried according to procedures described in the literature. ^{1}H NMR spectra were recorded with a Bruker Avance DMX 600 spectrophotometer. Scanning Electron Microscopy (SEM) investigations were carried out on a JEOL 6390LV instrument. UV−vis spectra were taken on a HICITHI UH5300 spectrophotometer. Thermogravimetric analysis (TGA) was taken on a METTLER TG/DSC1/1600 instrument. Rheological testing was performed on MCR102 Advanced Rheology Expanded Systems. X-ray diffraction (XRD) measurements were carried out on a Bruker D2 PHASER instrument. The surface area was determined by Braunuer-Emmet-Teller (BET) method using a Micromeritics TriStar II Plus 3030 instrument. Liquid nitrogen was used to measure the isotherms of N_2 adsorption and desorption at 77K.

Synthesis of hydrogel: All supramolecular polymer materials were synthesized according to the previously reported literatures.[S1,S2] By simply mixing **WP5** with different molar ratios of **PSS** at room temperature, pillar[5]arene-based bulk supramolecular hydrogel were obtained. For example, **WP5** (226 mg, 0.1 mmol) and **PSS** (206 mg, 1 mmol) were added into a 2 mL reagent bottle, and then 0.2 mL of water was added. Stir to mix thoroughly, it was left overnight at room temperature to complete the gelation process to obtain **SPH-1**.

2. Chemical structures of WP5, M and PSS

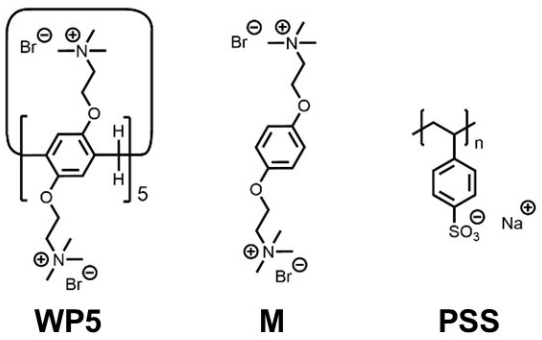

Fig. S1 Chemical structures of **WP5**, **M** and **PSS**.

3. Macroscopic pictures of WP5- and M-based supramolecular polymers

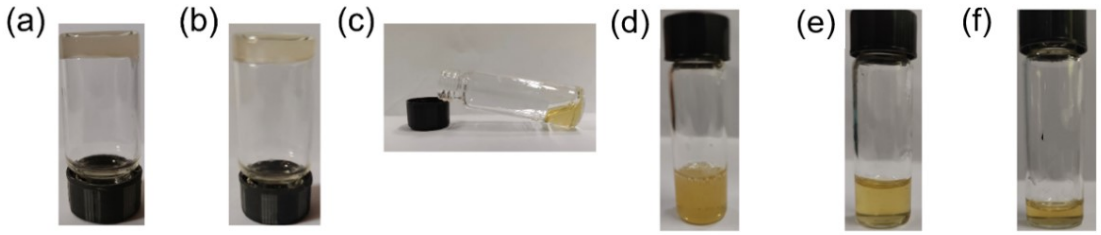

Fig. S2 Macroscopic Pictures: (a) **SPH-1**, (b) **SPH-2**, (c) **SPH-3**, (d) **M1**, (e) **M2** and (f) **M3**.

4. ^{1}H NMR characterization of the WP5-based supramolecular polymer

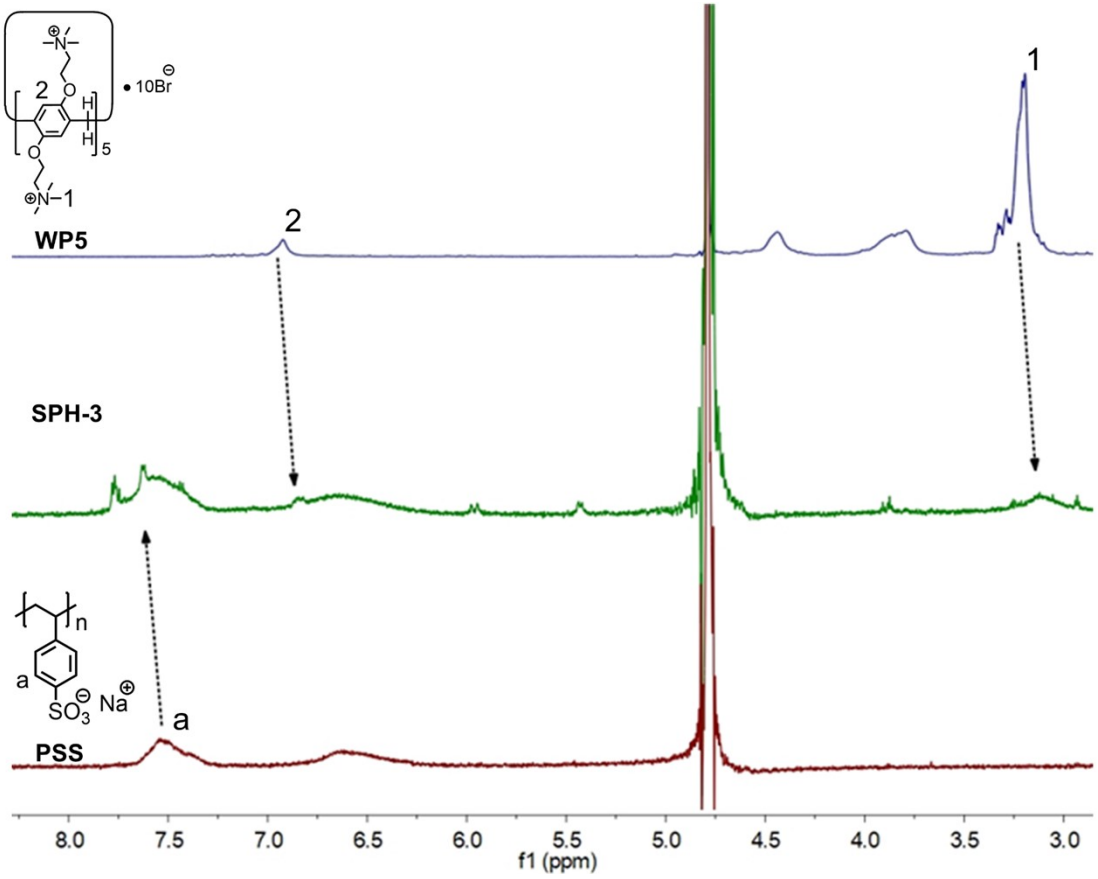

Fig. S3 Partial ^{1}H NMR spectra (600 MHz, D_2O, 298 K) of (a) **WP5** (5.00 mM), (b) **SPH-3 (**the molar ratio of (-$N(CH_3)_3^+$)/SO_3^- is 1:10**)** (5.00 mM) and (c) **PSS** (5.00 mM).

5. Water content analysis of hydrogel SPH-1

Table S1. Water content analysis.

W_d	W_w	Water content
24.53 mg	14.75 mg	66.3%
26.77 mg	15.16 mg	76.6%
38.85 mg	22.16 mg	75.3%
		Average: 72.7%

where W_s (mg) and W_d (mg) are represent the masses of the swollen hydrogel and the dried hydrogel, respectively. The water content was determined from the average (72.7%) of three measurements.

6. TG Analysis

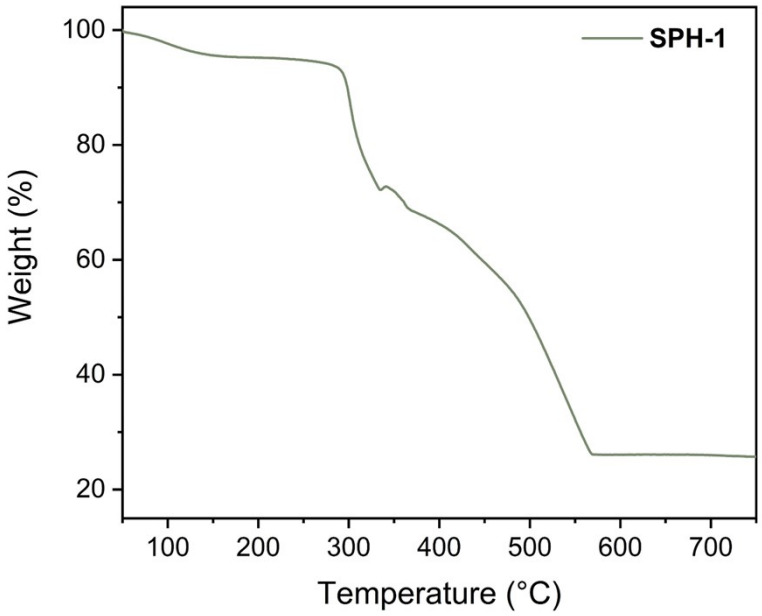

Fig. S4 Thermogravimetric analysis results of **SPH-1**.

7. Porosity and surface area measurements for SPH-1

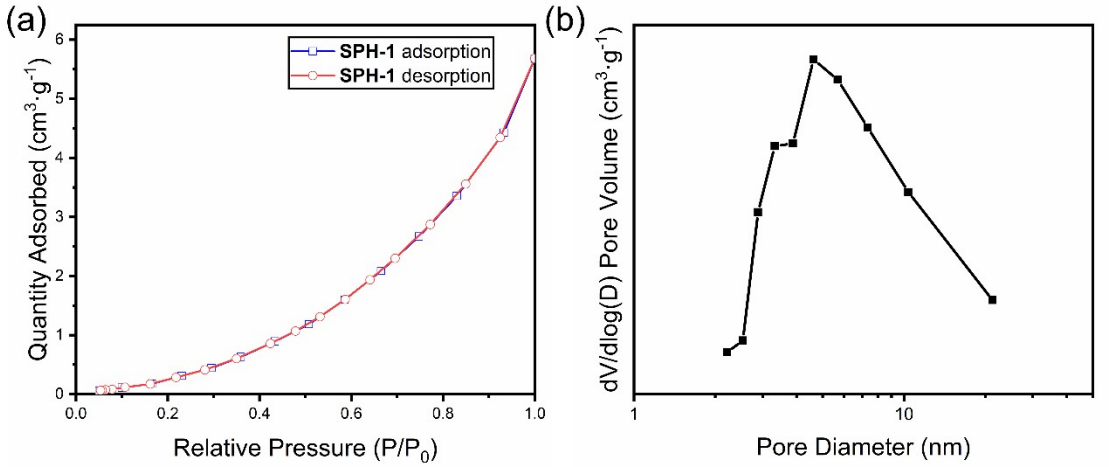

Fig. S5 (a) N_2 adsorption and desorption isotherm and (b) the pore size distribution of **SPH-1**.

8. XRD patterns

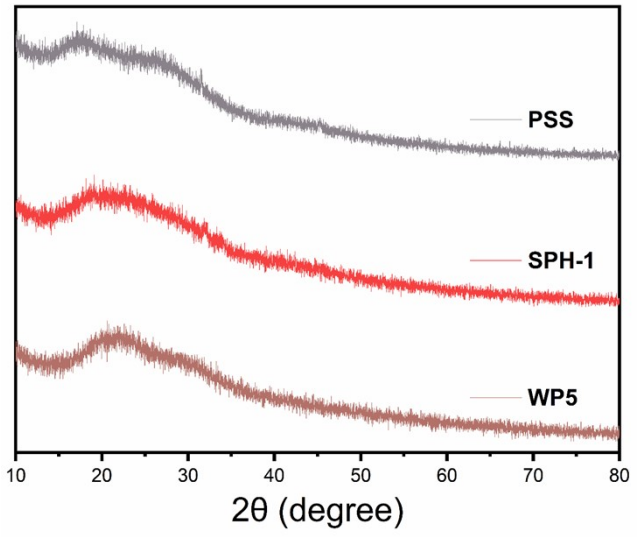

Fig. S6 XRD patterns of **PSS** and **SPH-1** and **WP5**.

9. Adsorption data of SPH-1 and SPH-2

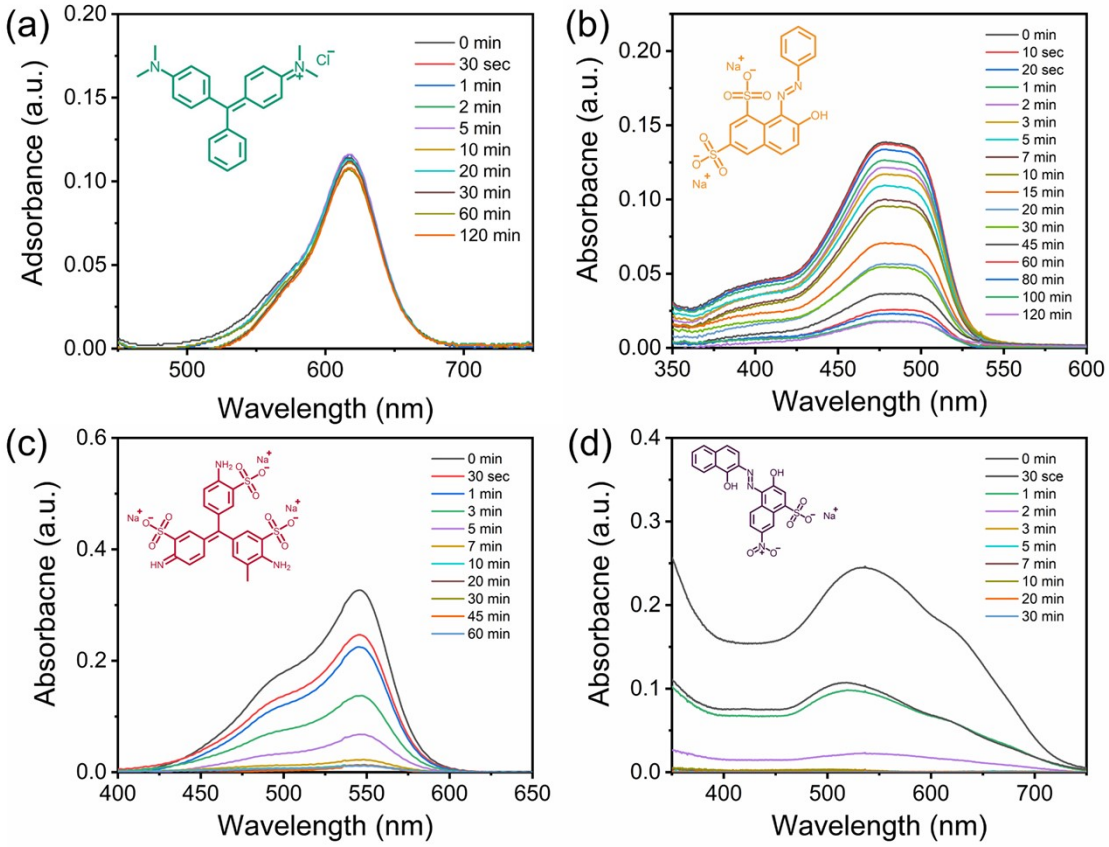

Fig. S7 Time-dependent changes in UV−vis spectra of (a) MG, (b) MO, (c) AF by **SPH-1** at 10-fold dilution. Time-dependent changes in UV−vis spectra of (d) EBT by **SPH-1**.

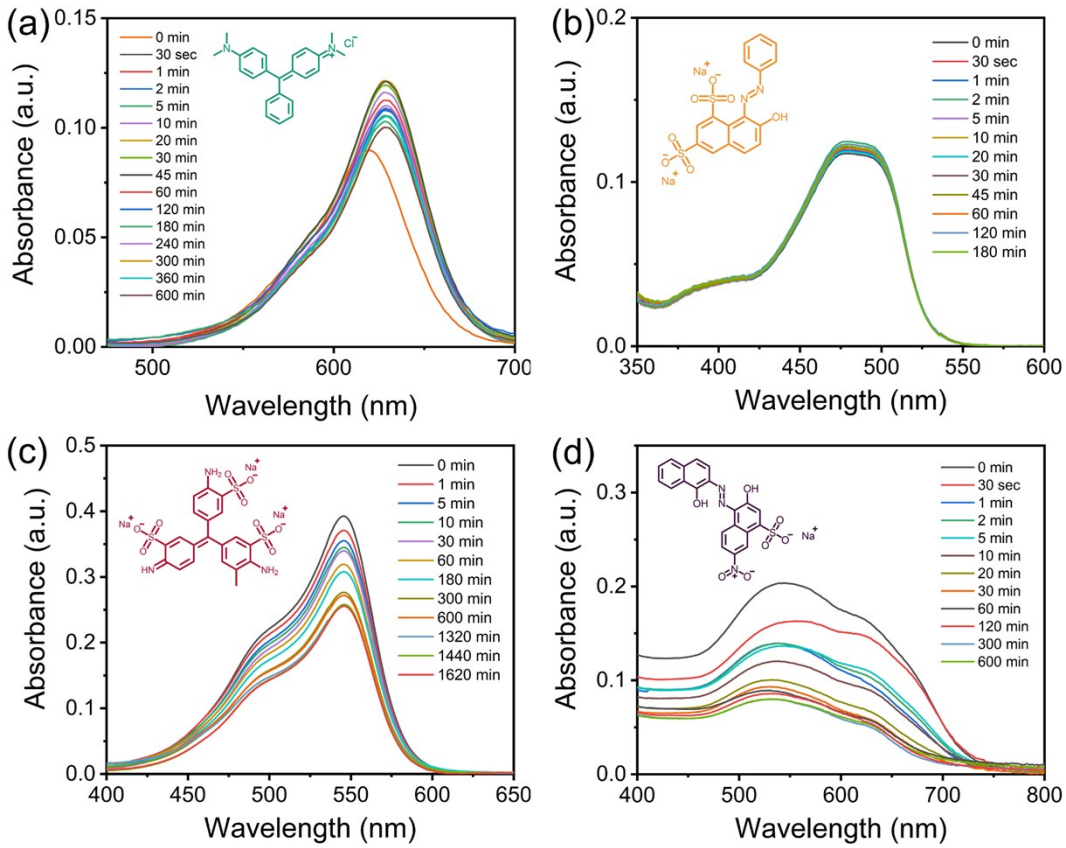

Fig. S8 Time-dependent changes in UV−vis spectra of (a) MG, (b) MO, (c) AF by **SPH-2** at 10-fold dilution. Time-dependent changes in UV−vis spectra of (d) EBT by **SPH-2**.

10. Adsorption kinetics

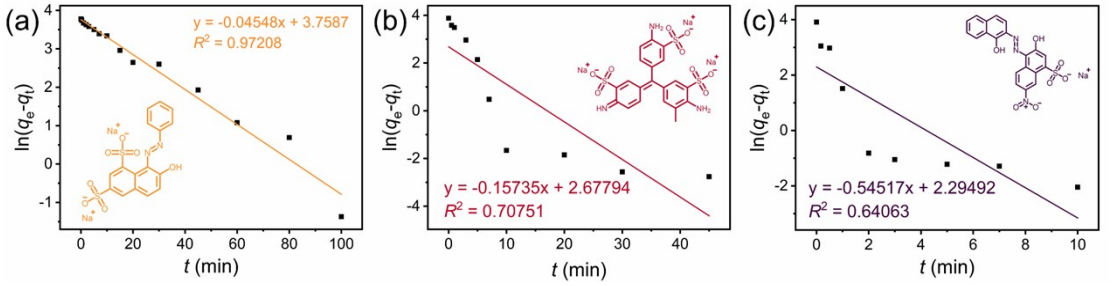

Fig. S9 The pseudo-first-order plots of **SPH-1** with (a) OG, (b) AF and (c) EBT.

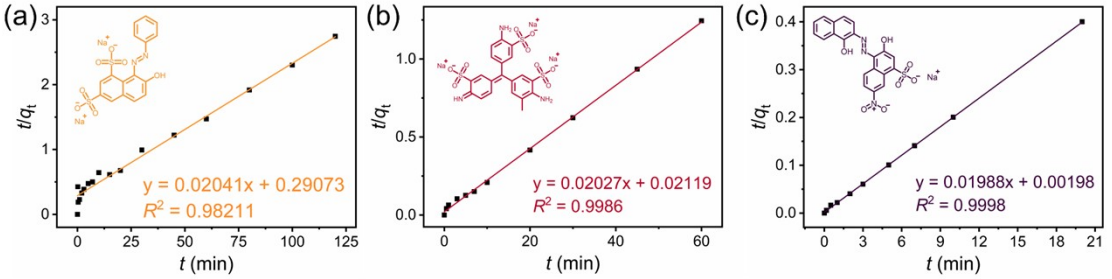

Fig. S10 The pseudo-second-order plots of **SPH-1** with (a) OG, (b) AF and (c) EBT.

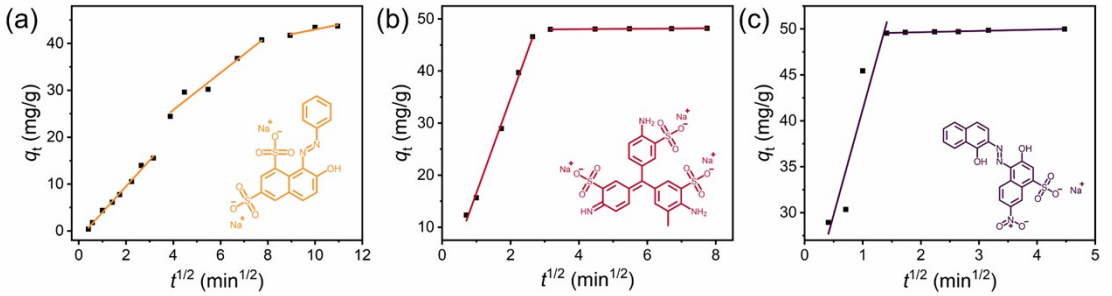

Fig. S11 The Weber and Morris plots of **SPH-1** with (a) OG, (b) AF and (c) EBT.

11. Adsorption isotherms

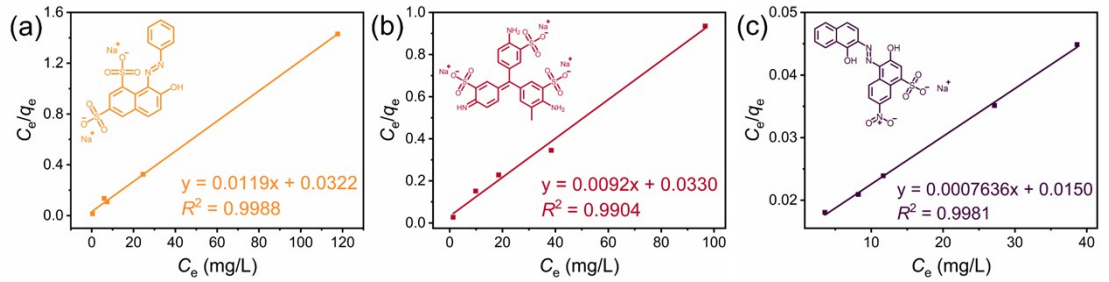

Fig. S12 The Langmuir model plots of **SPH-1** with (a) OG, (b) AF and (c) EBT.

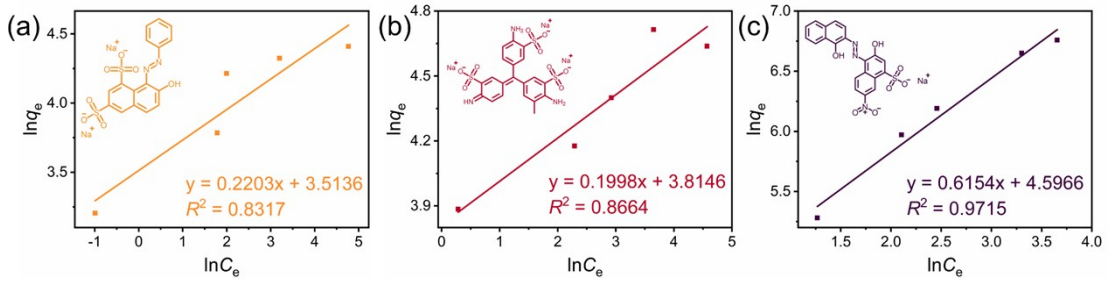

Fig. S13 The Freundlich model plots of **SPH-1** with (a) OG, (b) AF and (c) EBT.

12. Effect of ionic strength on adsorption of EBT

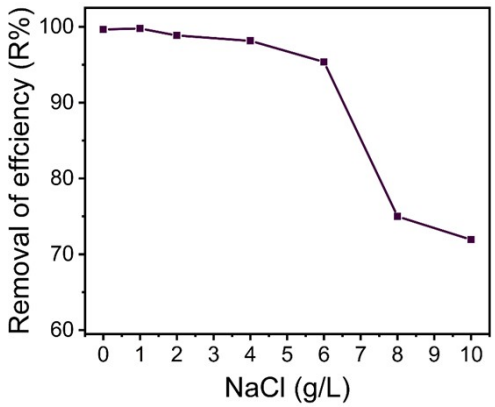

Fig. S14 Effect of electrolyte (NaCl) strength on the removal of EBT by **SPH-1**.

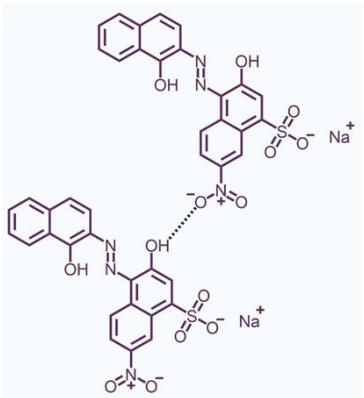

Fig. S15 Representation of EBT molecules dimerization in the presence of NaCl.

13. Effect of pH on adsorption of EBT

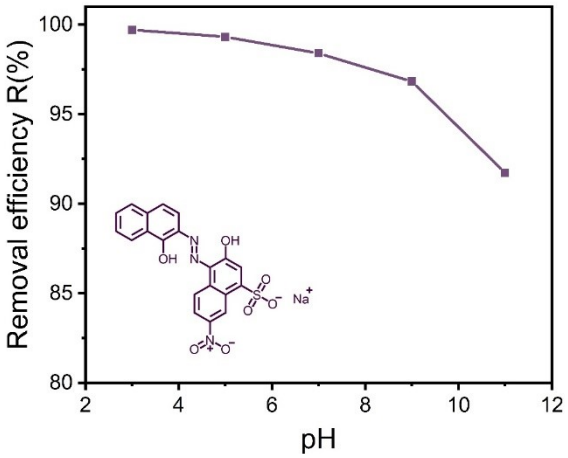

Fig. S16 Effect of pH on the removal of EBT by **SPH-1** (T = 25.0 °C, C_0 = 50 mg/L, and pH range of 2–10).

14. pH_{PZC} of SPH-1.

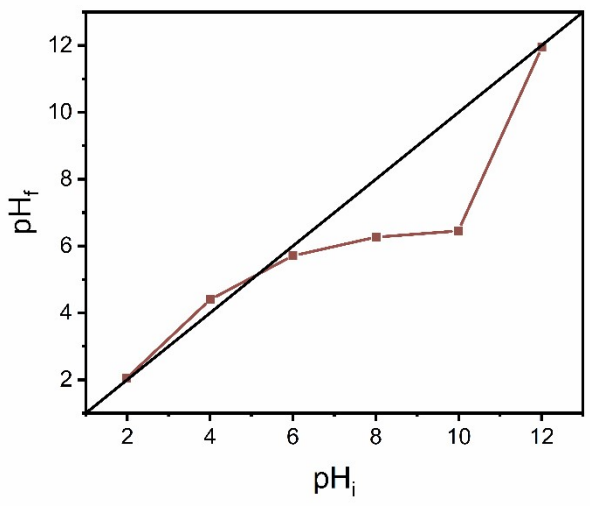

Fig. S17 pH_{PZC} of **SPH-1**.

15. Adsorption data of SPH-1 with EBT at PH = 3

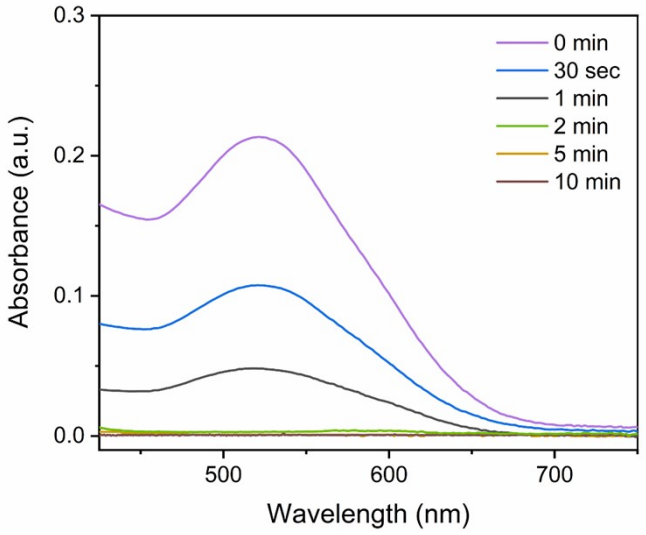

Fig. S18 Time-dependent changes in UV−vis spectra of EBT by **SPH-1** at pH = 3.

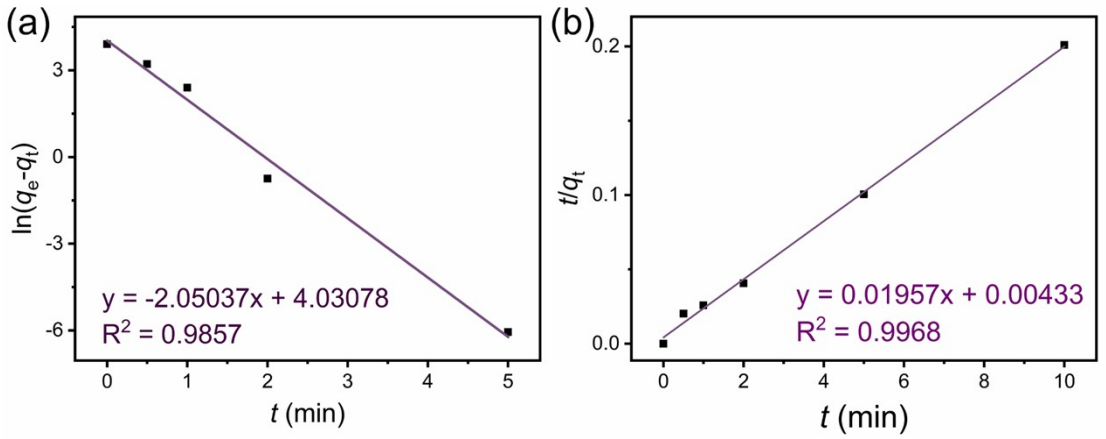

Fig. S19 The pseudo-first-order plots of **SPH-1** with EBT at pH = 3. (b) The pseudo-second-order plots of **SPH-1** with EBT pH = 3.

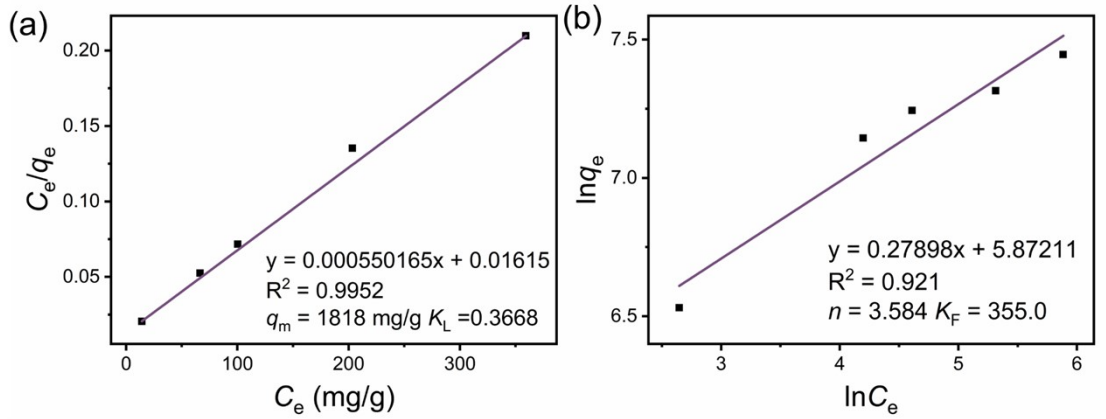

Fig. S20 The Langmuir model plots (a) and the Freundlich model plots (b) of **SPH-1** with EBT at pH = 3.

16. Adsorption studies of EBT dye in real samples

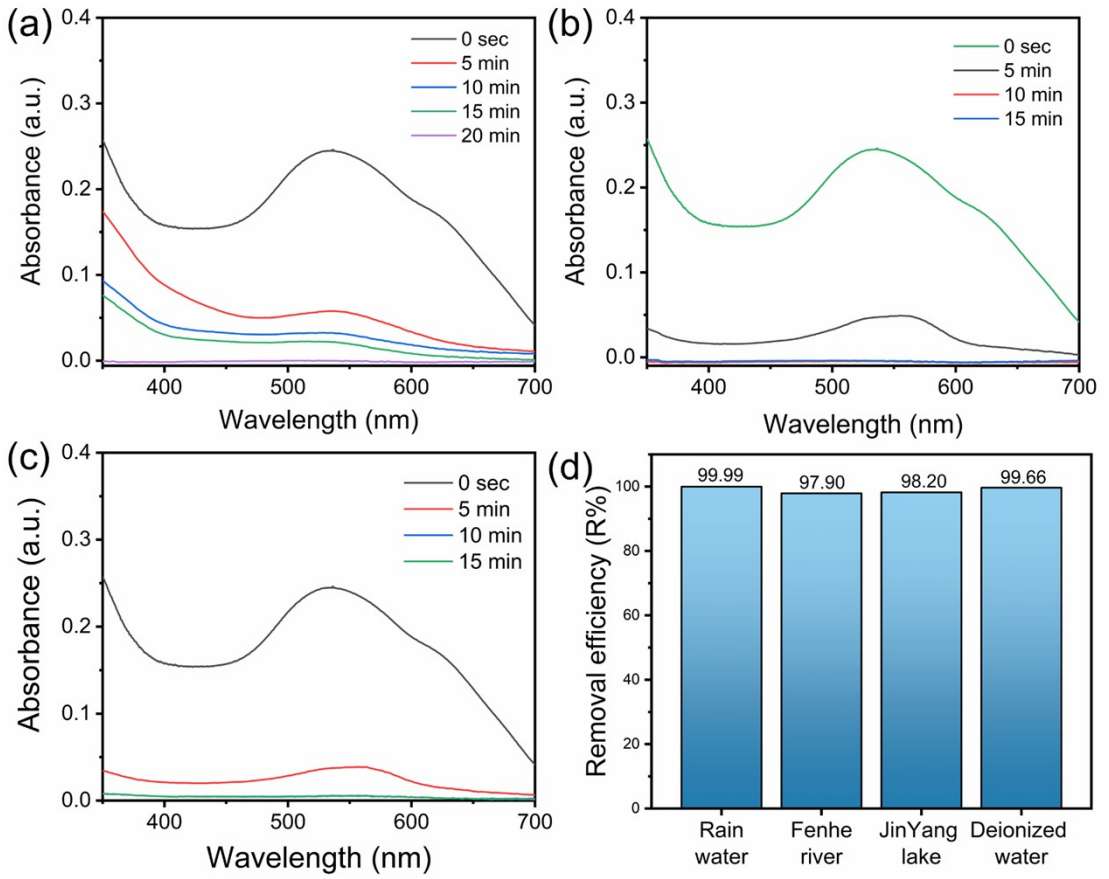

Fig. S21 Percentage removal of EBT dye in various real water samples.

17. Selective adsorption

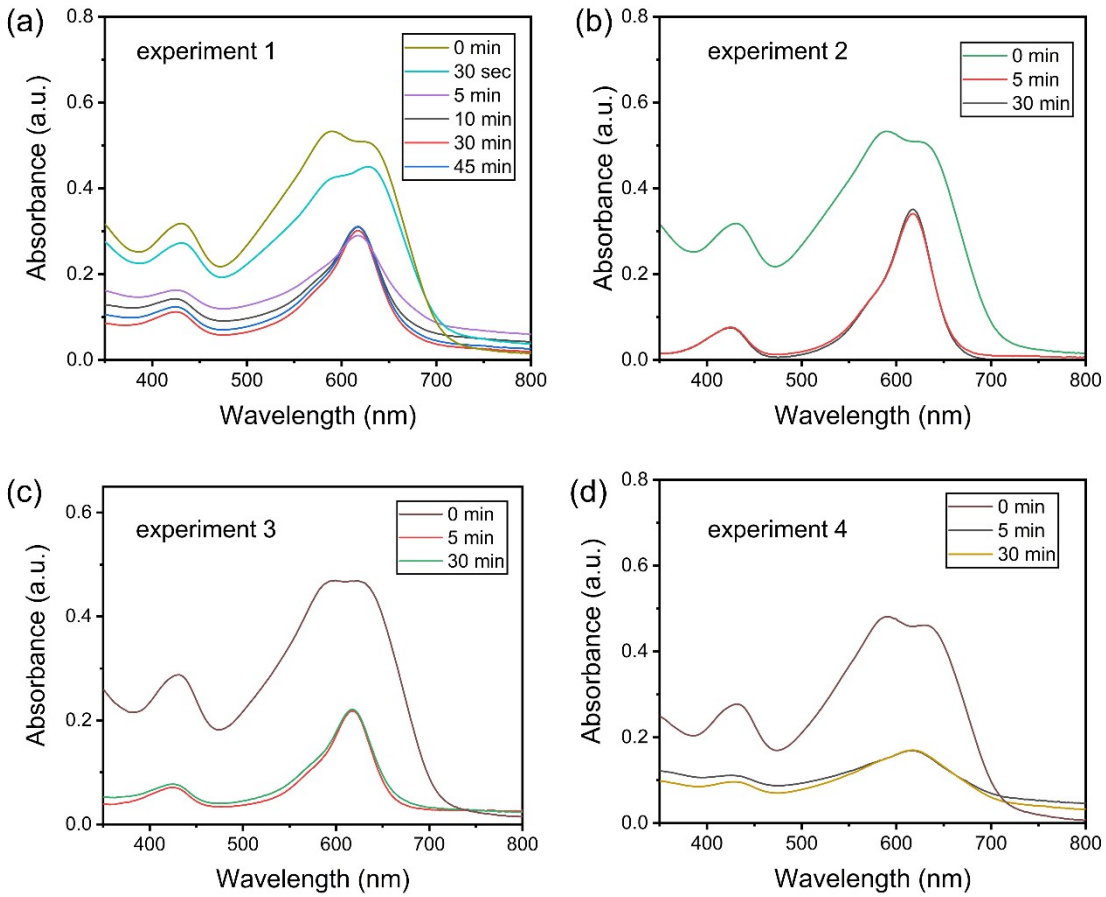

Fig. S22 The UV–vis spectra of the mixed solution of EBT and MG before and after adsorption by **SPH-1** by four times. The initial concentration of EBT and MG was 100 mg/L.

18. Activated carbon adsorption data with EBT

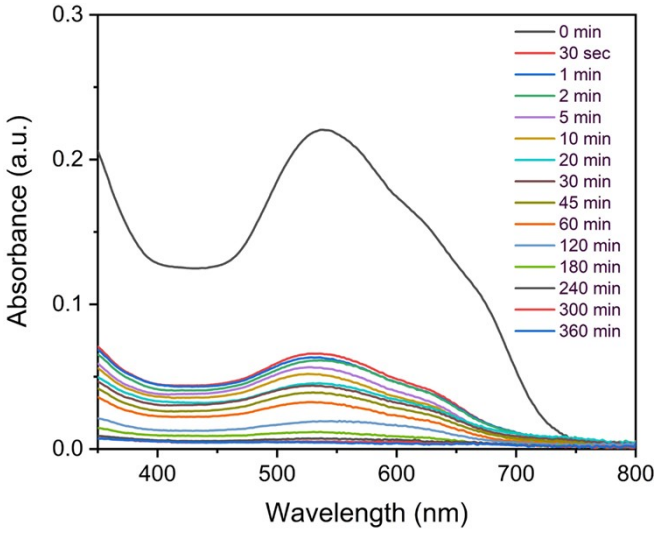

Fig. S23 Time-dependent changes in UV−vis spectra of EBT by activated carbon.

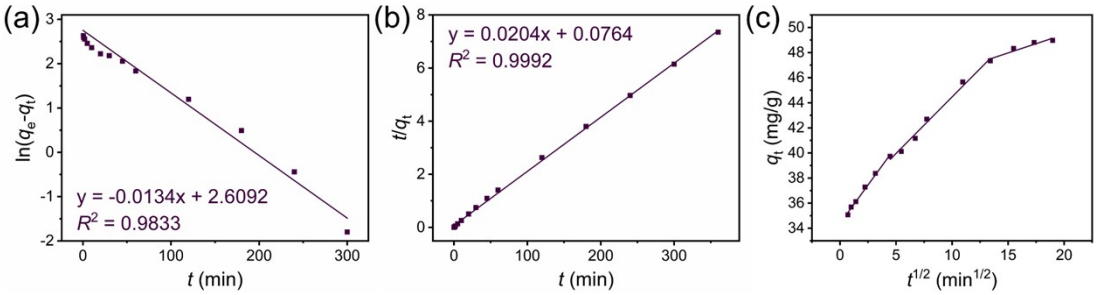

Fig. S24 (a) The pseudo-first-order plots of activated carbon with EBT. (b) The pseudo-second-order plots of activated carbon with EBT. (c) The Weber and Morris plots of activated carbon with EBT.

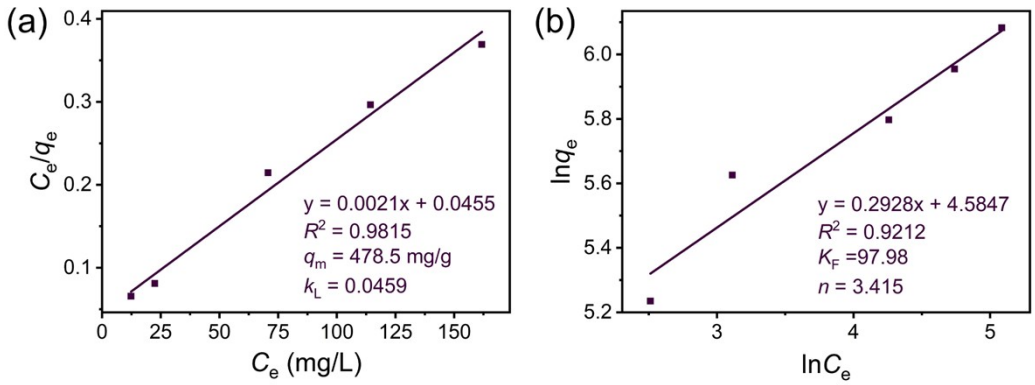

Fig. S25 The Langmuir model plots (a) and the Freundlich model plots (b) of activated carbon with EBT.

References

(1) Hua, B.; Shao, L.; Yu, G.; Huang, F. Fluorescence indicator displacement detection based on pillar[5]arene-assisted dye deprotonation. *Chemical Communications* **2016**, *52* (65), 10016-10019.

(2) Gui, J.-C.; Yan, Z.-Q.; Peng, Y.; Yi, J.-G.; Zhou, D.-Y.; Su, D.; Zhong, Z.-H.; Gao, G.-W.; Wu, W.-H.; Yang, C. Enhanced head-to-head photodimers in the photocyclodimerization of anthracenecarboxylic acid with a cationic pillar[6]arene. *Chinese Chemical Letters* **2016**, *27* (7), 1017-1021.